Thermionic properties of lutetium borides single crystals

D.A.Voronovich, A.A.Taran, N.Yu.Shitsevalova*, G.V.Levchenko*, V.B.Filipov*

National Aerospace University "Kharkiv Aviation Institute", 17 Chkalov Str., 61070 Kharkiv, Ukraine
*I. Frantsevich Institute for Problems of Material Science, National Academy of Sciences of Ukraine, 3 Krzhyzhanovsky Str., 03680 Kyiv 142, Ukraine

Results of the LuB_{12} (100), (110), (111), LuB_4 (001), LuB_2 (001) thermionic properties study in the temperature range $T = 1200...1960$ K at $p \leq 10^{-4}$ Pa pressure are presented. The correlation between structure and composition of the lutetium borides single-crystal samples and their thermionic properties are shown. The electron work function anisotropy of the LuB_{12} low-index planes are determined by the lutetium and boron atoms reticular density and the electric dipole moment of the unreconstructed (100), (110), (111) planes of the UB_{12} type lattice structure.

Представлены результаты исследований термоэмиссионных свойств LuB_{12} (100), (110), (111), LuB_4 (001), LuB_2 (001) в температурном диапазоне $T = 1200...1960$ К при давлении $p \leq 10^{-4}$ Па. Показана взаимосвязь структуры и состава монокристаллических образцов боридов лютеция с их термоэмиссионными характеристиками. На основе теоретических расчетов ретикулярной плотности ионов металла и бора и электрического дипольного момента неперестроенных поверхностей (100), (110), (111) решетки типа UB_{12} объяснена анизотропия работы выхода электрона низкоиндексных плоскостей монокристаллов LuB_{12}.

Термоемісійні властивості монокристалів боридів лютецію. *Д.О.Воронович, А.О.Таран, Н.Ю.Шіцевалова, Г.В.Левченко, В.Б.Філіпов.*

Представлено результати досліджень термоемісійних властивостей LuB_{12} (100), (110), (111), LuB_4 (001), LuB_2 (001) у температурному діапазоні $T = 1200...1960$ К при тиску $p \leq 10^{-4}$ Па. Показано взаємозв'язок структури і складу монокристалічних зразків боридів лютецію з їх термоемісійними характеристиками. На основі теоретичних розрахунків ретикулярної густини іонів металу і бору та електричного дипольного моменту неперебудованих поверхонь (100), (110), (111) гратки типу UB_{12} пояснено анізотропію роботи виходу електрона низькоіндексних площин монокристалів LuB_{12}.

1. Introduction

Four binary compounds: lutetium di-, tetra-, dodeca- and hectoboride (LuB_2, LuB_4, LuB_{12} and LuB_{66}, accordingly) — are known among Lu–B systems [1]. Thermionic emission properties were studied only for LuB_{12}, and the investigations have been performed with polycrystalline samples [2].

Earlier the thermionic properties anisotropy of low-index crystallographic planes of erbium dodecaboride ErB_{12} was experimentally investigated [3]. The boron and erbium reticular densities (d_r) (number of atoms

(ions) per unit area in any plane of a crystal lattice) in ErB_{12} low-index planes were considered in [3] and it was shown that decreasing of electron work function for the ErB_{12} crystallographic planes in row $(100) \rightarrow (110) \rightarrow (111)$ correlates with the following decreasing of reticular densities $d_r(B)/d_r(Er)$ ratio: $4 \rightarrow 2 \rightarrow 0$. Taking into account that LuB_{12}, as well as ErB_{12}, crystallizes in a face-centered cubic lattice of UB_{12} crystal structure type (space group $Fm\overline{3}m{-}O_h^5$) [4] it can be supposed that decreasing of the electron work function for the LuB_{12} low-index planes is similar to ones of the corresponding ErB_{12} planes. Reasons of the thermionic properties anisotropy for dodecaborides with UB_{12}-type lattice are unclear.

Lanthanum hexaboride is the most studied thermionic material among borides. Its lower values of the electron work function for (100) and (110) planes in comparison with the (111) one are caused by electric dipole moment of dipoles formed from surface positively charged lanthanum ions and the nearest to them negatively charged B_6 octahedra [5, 6]. The surface of LaB_6 (100) consists of La atoms layer, under it the octahedra B_6 layer is situated at a distance of 2.08 Å (half of the LaB_6 lattice constant). The surface atoms of La in LaB_6 (110) are displaced outwards at 1.66 Å in relation to the B_6 octahedra layer. Therefore the electric dipole moment of the LaB_6 (110) surface layer is less than of the (100) one. The surface atoms of La in LaB_6 (111) are displaced outwards at 1.2 Å relative to their positions in the ideal lattice and situated at grade with the B_6 octahedra layer. And so the electric dipole moment of LaB_6 (111) surface layer equals zero. The greater is the electric dipole moment of the LaB_6 surface layer, the less the electron work function φ is.

It is very likely that the thermionic properties anisotropy of LuB_{12} single crystal unreconstructed surfaces also is governed by different values of the surface electric dipole moment.

The aims of this work are:
— experimental research of the electron work function temperature dependences of LuB_{12} (100), (110) and (111); LuB_4 (001), LuB_2 (001) at $p \leq 10^{-4}$ Pa pressure in the temperature range $T = 1200...1960$ K;
— study of the thermionic properties anisotropy of the LuB_{12} low-index planes;

— calculation of the electric dipole moment of the unreconstructed (100), (110), (111) LuB_{12} surfaces;
— measurement of the evaporation rate of lutetium boride single crystals;
— investigation of interrelation between structure and composition of lutetium borides with their thermionic properties before and after thermionic tests.

2. Experimental

Lutetium borides LuB_{12}, LuB_4 and LuB_2 investigated in this study were grown by crucible free inductive zone melting. The preparation peculiarities and structure examination of the produced single crystals are presented in [7]. The experimental equipment and thermionic properties research procedure of the lutetium borides single-crystal samples were the same as for ErB_{12} single crystals [3].

The evaporation rate G of the investigated lutetium borides single crystals was determined by rate of a weight loss obtained as a difference between the specimen weight before and after heating.

The evaporation rate of the most substances may be expressed by the following relation

$$\lg G = C - 0.5\lg T - (B/T),$$

where G is in grams per square centimeter per second at temperature T in kelvins, C and B are empirical constants [8]. For example, for LaB_6 $C = 13$ and $B = 36850$ K. With increasing temperature the evaporation rate significantly increases and the main weight loss takes place at high temperatures. At the same time a prolonged heating at lower temperatures may result in the same values of a weight loss. Therefore hereinafter G is given either after the highest working temperatures for LuB_{12} (100), LuB_4 (001), or after the prolonged heating at the lower temperatures for LuB_{12} (111) and (110), LuB_2 (001). The relative error of G determination is 30 %.

3. Results and discussion

It is known that temperature dependences of the electron work function of the most studied borides are described by linear functions in a certain temperature range [9]. Therefore it we can expect that φ(T) dependences of the studied lutetium borides specimens will be described by linear functions in the certain temperature ranges too.

It is also known that metal content in emitting surface plays the main role in thermionic activity of boride cathodes. The planes (001) of LuB$_4$ and LuB$_2$ lattices are composed only of lutetium atoms [10]. Although anisotropy of the LuB$_4$ and LuB$_2$ thermionic properties has not yet been studied it is supposed that the LuB$_4$ and LuB$_2$ highest thermionic currents will be just for (001) plane.

At first let's consider results of the study of LuB$_{12}$ single-crystal thermionic. Measurements of the LuB$_{12}$ (100), (110) and (111) thermionic current were performed with increasing temperature in the range of $T = 1220...1960$ K during 7 h. The $\varphi(T)$ dependences calculated by use of current values are presented in Fig. 1. The equations describing $\varphi(T)$ dependence for different low-index crystallographic planes of LuB$_{12}$, values of the thermionic current densities j and according φ at 1800 K, the rates of evaporation at 1900 K and calculated values of j for polycrystalline LuB$_{12}$ by use of data from [2] are presented in Table 1. As in the case of polycrystalline LuB$_{12}$ the electron work function temperature dependences $\varphi(T)$ for LuB$_{12}$ (100), (110), (111) are described by the linear functions in the certain temperature ranges.

As can be seen from the experimental results the electron work function decreases in the series (100) → (110) → (111). It is in a good agreement with decreasing of $d_r(\text{B})/d_r(\text{Me})$ ratio for low-index planes of UB$_{12}$ — type lattice in the same series [3]. The boride electron work function anisotropy is conditioned on φ dependence on the surface $d_r(\text{B})/d_r(\text{Me})$ ratio and the electric dipole moment of the surface dipole per one metal ion [6]. The dipole contribution $\Delta\varphi_D$ to the electron work function is propor-
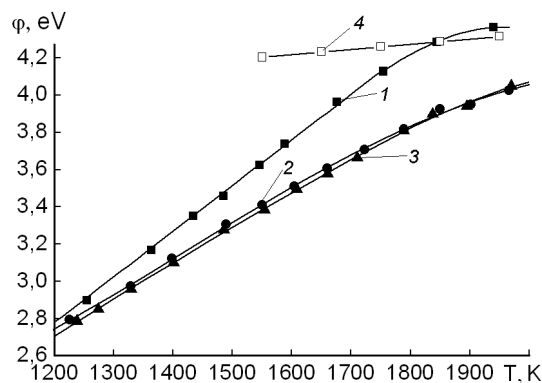

Fig. 1. Temperature dependences of LuB$_{12}$ electron work function: *1* — (100), *2* — (110), *3* — (111), *4* — polycrystal [2].

tional to reticular density of the metal ions d_r and normal component of the electric dipole moment of the surface dipole p_e per metal ion [11]:

$$\Delta\varphi_D = -\frac{d_r p_e}{\varepsilon_0},$$

$$p_e = \frac{q}{N}\sum_{i=1}^{N} r_i\cos\theta_i,$$

where $\varepsilon_0 = 8.85 \cdot 10^{-12}$ F·m^{-1} is the electric constant, q is the effective charge of a metal ion (in coulombs), N is the quantity of B$_{12}$ cubooctahedra nearest to the metal ion on the surface, r_i is the distance between metal ion and nearest ith B$_{12}$ cubooctahedron, θ_i is the angle between the direction from the metal ion to ith B$_{12}$ cubooctahedron and the surface normal **n**. Using LuB$_{12}$ three-dimensional modeling and its lattice parameter [4] it was obtained that the quantity of the B$_{12}$ cubooctahedra nearest to the metal ion is equal to 5, 4, 3 for

Table 1. Thermionic properties and evaporation rates of low-index crystallographic planes of lutetium dodecaboride

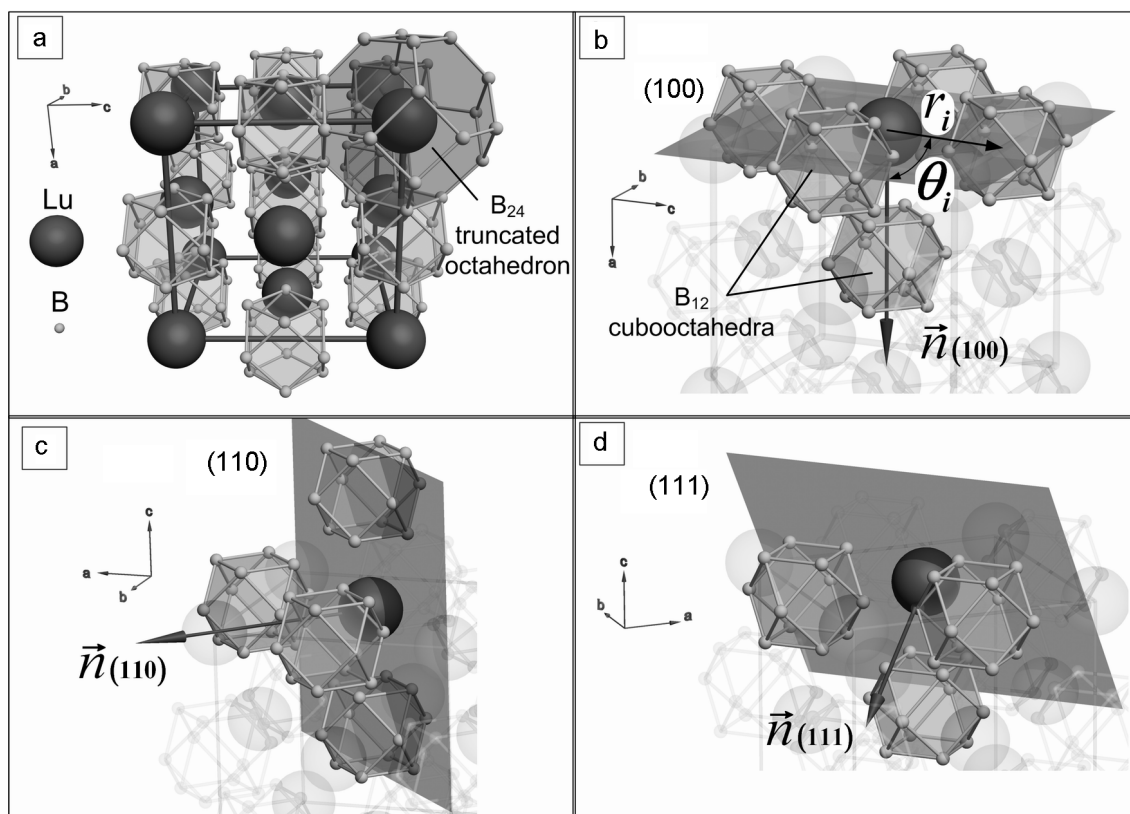| Characteristics	LuB$_{12}$			
	(100)	(110)	(111)	polycrystal [2]
$\varphi(T)$, eV	$-0.16 + 24.5\cdot10^{-4}T$	$0.49 + 18.8\cdot10^{-4}T$	$0.50 + 18.5\cdot10^{-4}T$	$3.77 + 2.8\cdot10^{-4}T$
T, K	1220...1800		1550...1950	
φ, eV ($T = 1800$ K)	4.25	3.87	3.83	4.27
j, A·cm^{-2} ($T = 1800$ K)	$4.9\cdot10^{-4}$	$5.7\cdot10^{-3}$	$7.4\cdot10^{-3}$	$4.3\cdot10^{-4}$
G, 10^{-7}kg·m^{-2}·s^{-1} ($T = 1900$ K, $p \sim 10^{-4}$ Pa)	25.3	9.4	14.4	—

Fig. 2. Fragments of 3D model of LuB_{12} crystal structure and its basal (100), (110), (111) planes centered on metal ion with the nearest to it B_{12} cubooctahedra both in plane and outside it: a — unit cell, b — (100), c — (110), d — (111).

each metal ion located in (100), (110) and (111) planes accordingly (see Fig. 2). Taking into account the metal ions reticular density from [3] and the lattice constant a (for LuB_{12} $a = 0.74646$ Å [4]) the value of $\Delta\varphi_D$ is obtained (Table 2). As it should be from calculations for the low-index planes of UB_{12}-type lattice a metal enrichment of crystallographic plane results in the surface electric dipole moment increase and the corresponding electron work function decrease. In particular $\Delta\varphi_D$ decrease for LuB_{12} in series (100) → (110) → (111) correlates with the electron work function decrease that has been observed experimentally

(Fig. 1). At the same time in spite of essential difference between $\Delta\varphi_D$ for (110) and (111) (Table 2), $\varphi(T)$ values for these planes are almost the same (Fig. 1). This is may be due to the fact that there is displacement of the near-surface Lu ions outward the surface that results in a difference in values of the electric dipole moment of surface dipoles in the real and ideal crystal structures. It is necessary to note the direct experimental measurements of p_e have not been performed to present day.

A deviation from the $\varphi(T)$ linear dependence takes place with increasing temperature above $T > 1800$ K for all low-index planes of LuB_{12} (Fig. 1). Earlier it was es-

Table 2. Some characteristics of low-index crystallographic planes of UB_{12}-type lattice

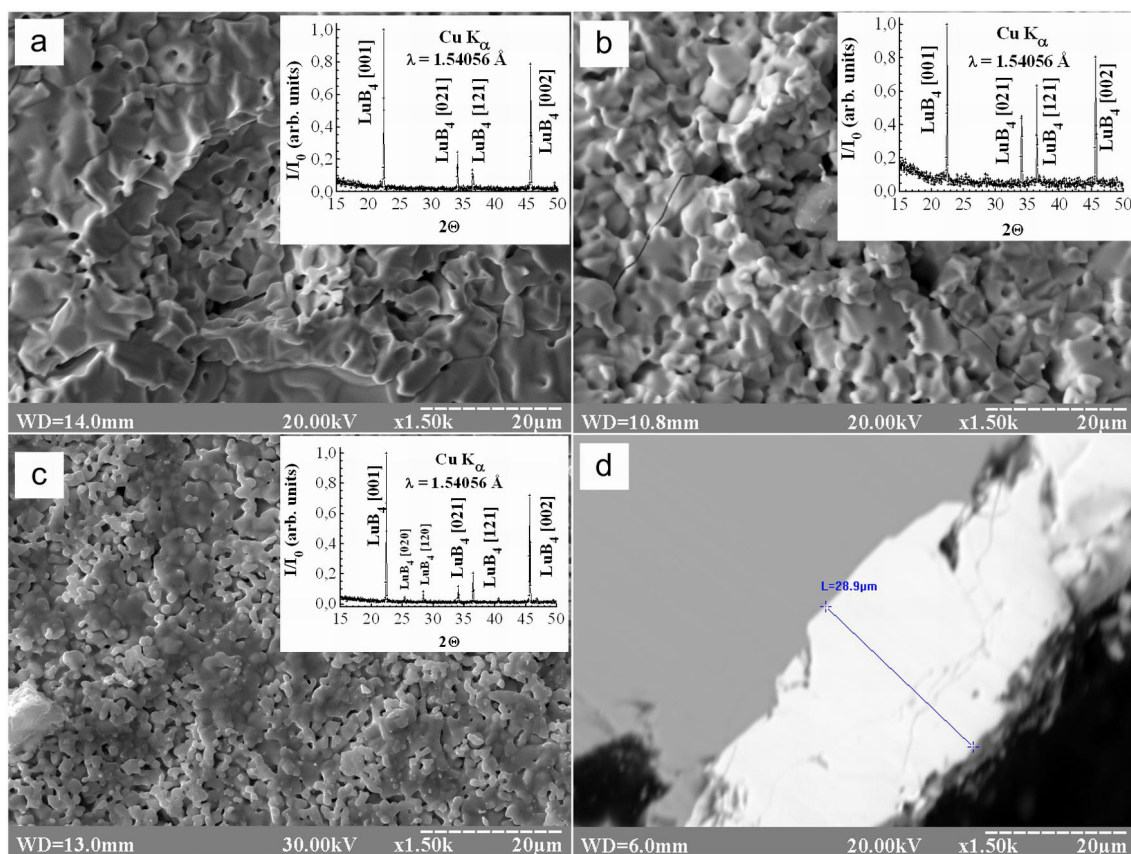| Crystallographic plane	Reticular density d_r, a^{-2}		$d_r(B)/d_r(Me)$	p_e, $q \cdot a$	$\Delta\varphi_D$, $q/\varepsilon_0 a$
	B	Me			
(100)	8	2	4	0.1	−0.2
(110)	$2\sqrt{2}$	$\sqrt{2}$	2	$\sqrt{2}/8$	−0.25
(111)	0	$2\sqrt{3}/3$	0	$\sqrt{3}/6$	−0.33

Fig. 3. SEM images of the samples surfaces covered by LuB_4 layer after thermionic investigations and corresponding X-ray diffraction patterns (inserts): a — [100], b — [110], c — [111], d — longitudinal section of LuB_{12} [111] cathode with near-surface layer LuB_4 (details are in the text).

tablished [10] that on LuB_{12} heating in the range of $T = 1400...1800$ K the surface restructuring takes place with LuB_4 phase formation in the surface layer due to preferential boron evaporation. In doing so dislocations of the crystal lattice can be centers of the LuB_4 phase nucleation. Taking into account the dislocations low density in the studied LuB_{12} single crystals (less than 10^6 cm^{-2}, i. e. an average distance between adjacent dislocations equals ~ 10 μm [7]), we can assume that at the initial heating of LuB_{12} single crystals in the range of $T = 1400...1800$ K the emitting surface have consisted of the starting LuB_{12} phase and LuB_4 phase appeared during heating. As shown in [3] the nonlinearity φ(T) of this surface consisting of tetra- and dodecaboride can be caused due to extension of the surface area with tetraboride with increasing temperature (or during prolonged annealing).

After thermionic current measurements in the range of $T = 1220...1960$ K during 7 h the additional annealing of the LuB_{12} single-crystal samples with different orien-tation was performed to establish how modification of the structure and phase composition of the surface affects on the thermionic properties. Annealing duration and temperature values were $t = 10$ h, $T = 1550$ K for LuB_{12} (100); $t = 40$ h, $T = 1900$ K for LuB_{12} (110) and (111). It was cleared up that the annealing results in formation of the lutetium tetraboride layer with coral-like structure and ≈30 μm thick at the starting LuB_{12} surface (Fig. 3).

The φ(T) temperature dependences of such LuB_{12} samples with the formed LuB_4 surface layer are presented in Fig. 4, a. These dependences were obtained both at the temperature increase and decrease. Due to phase transformation $LuB_{12} \rightarrow LuB_4$ and structure restructurings of the near-surface layer the electron work function decreased compared with the starting LuB_{12}. For instance the electron work function for the starting LuB_{12} (100) decreased by 0.88 eV at $T = 1900$ K. Irrespective of the initial orientation of the LuB_{12} single-crystal samples after annealing their φ(T) are described by the linear functions.

After annealing all samples of the starting LuB_{12} were characterized by different values of the electron work function that is apparently determined by two factors: by various LuB_4 crystallographic facets on the emitting surface (inserts on Fig. 3) to a greater extent; by effective area enlargement of the emitting surface owing to its coral-like structure to a lesser extent.

It is known [6] that activation energy of lanthanum atoms evaporation for the LaB_6 low-index crystal faces is almost the same. At the same time the activation energy of boron atoms evaporation depends on the surface orientation. We suppose that the similar dependence takes place for LuB_4 crystal too i.e. the activation energy of the boron atoms evaporation depends on the emitting surface orientation that results in thermal faceting of the emitting surface and as a consequence the different electron work function of the LuB_{12} samples covered by LuB_4 layer after annealing.

Next stage of the researches was related with the current density measurements and electron work function calculation for (001) plane of the specially grown LuB_4 [001] single-crystal. At first the thermionic properties of LuB_4 (001) were investigated with increasing temperature in the range of $T = 1240...1910$ K during 3 h. The $\varphi(T)$ dependence of the starting LuB_4 (001) (Fig. 4, b) is described by nonlinear function and themselves the starting φ values differ from the φ values of LuB_4 formed on the annealed LuB_{12} surface (Fig. 4, a).

The obtained difference in the φ values is explained by the structure and phase composition modification of the LuB_4 [001] crystal under heating in vacuum. Due to the preferential boron evaporation $LuB_4 \rightarrow LuB_2$ phase transformation took place [10]. Subsequent LuB_4 [001] annealing at $T = 1500$ K during 8 h resulted in increase of the thermionic current. After annealing the LuB_4 $\varphi(T)$ dependence had loop — shape form with increasing temperature to 1900 K and subsequent its decrease (Fig. 4, b). This $\varphi(T)$ peculiarity may be explained by assumption that lutetium flow rises from the bulk towards the emitting surface with increasing temperature, at the same time boron evaporation prevails from the surface that results in lutetium enrichment of the surface and the thermionic current increases accordingly. With temperature decreasing the thermionic current values are higher than at the previous temperature in-
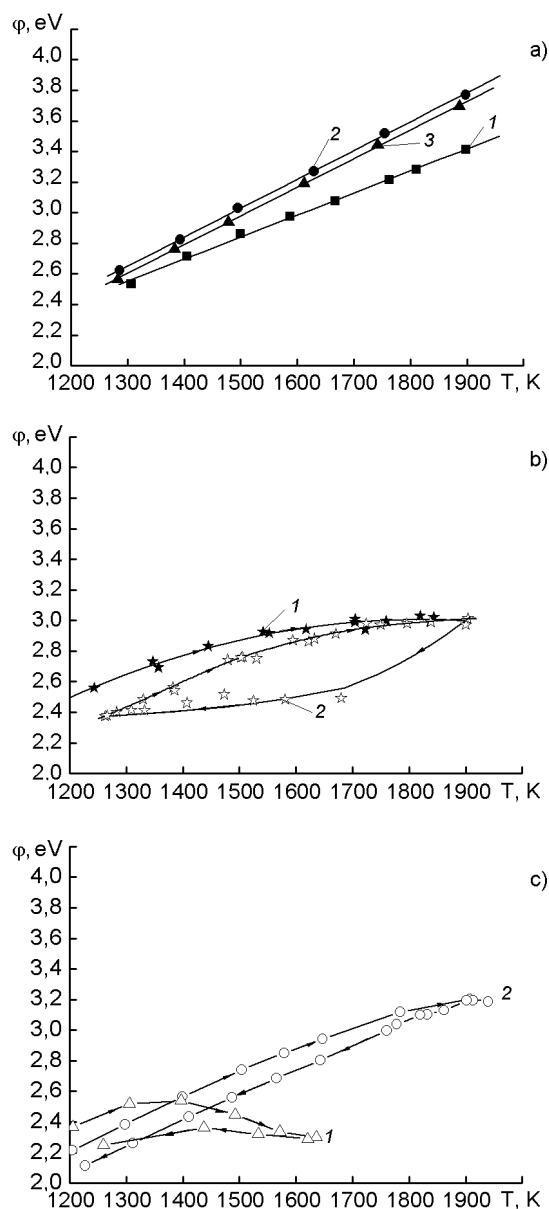

Fig. 4. Temperature dependences of the electron work function: a — LuB_{12} samples after annealing covered by LuB_4 layer: *1* — [100], *2* — [110], *3* — [111];

b — LuB_4 [001] sample: *1*—source, *2* — after annealing covered by LuB_2 layer; c — LuB_2 [001] sample: *1* — source, *2* — after annealing.

crease due to the "frozen" heightened content of lutetium at the surface. According to X-ray phase and microprobe analyses the LuB_4 surface layer after annealing consisted of polycrystalline LuB_2 only (Fig. 5, a).

It should be noted that $LuB_4 \rightarrow LuB_2$ phase transformation took place not only at the surface but also in the volume with formation of the like-directed LuB_2 lamellae
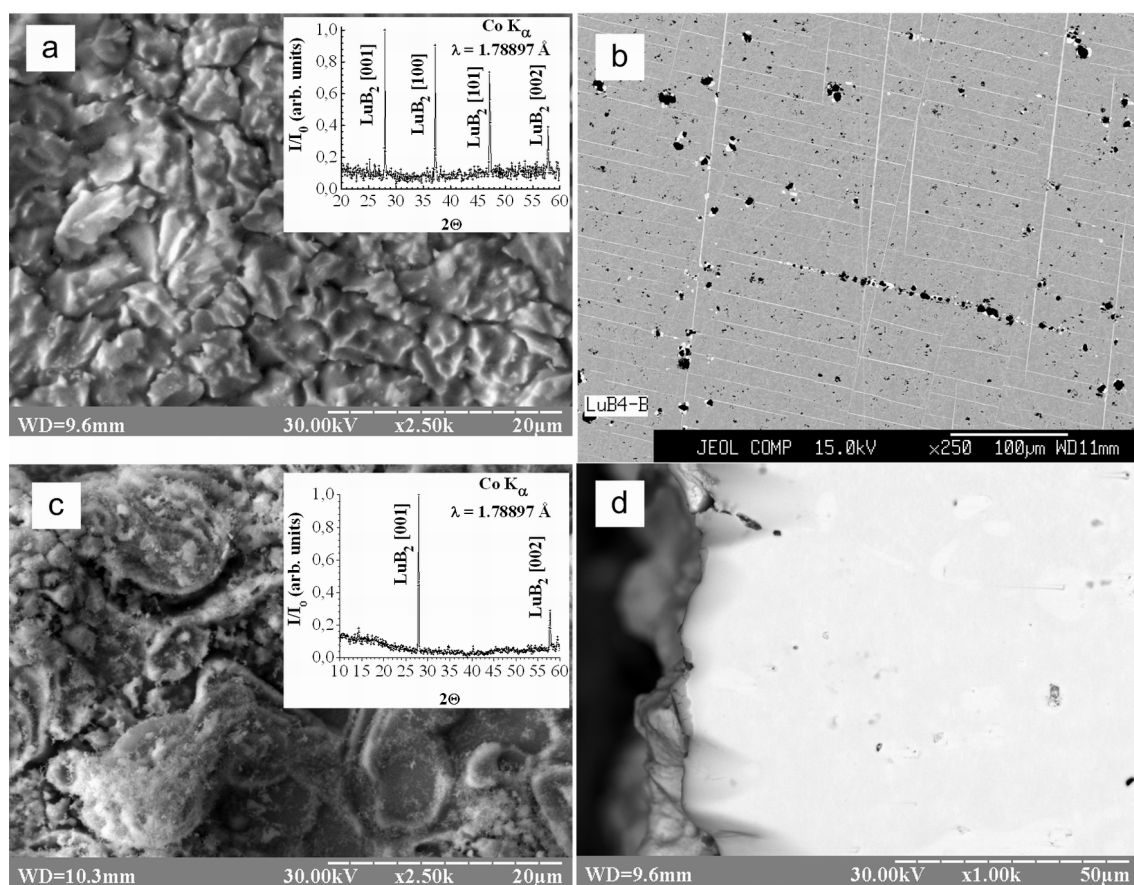
Fig. 5. SEM images and X-ray diffraction patterns (insert): a — LuB_2 at surface of LuB_4 [001], b — longitudinal section of LuB_4 [001] with LuB_2 lamellae, c — LuB_2 (001) after annealing, d — cross—section of LuB_2 [001] near-surface layer.

(Fig. 5, b). Therefore the thermionic current of the starting LuB_4 sample after annealing is defined both the LuB_2 thermionic properties and boron diffusion towards the emitting surface through the LuB_2–LuB_4 interface boundary and along interface boundaries of the LuB_2 lamellae from LuB_4 volume. The LuB_4 (00$\bar{1}$) evaporation rate equal $G = 8.9 \cdot 10^{-7}$ kg·m^{-2}·s^{-1} at $T = 1900$ K was less than one for the LuB_{12} low-index planes of (see Table 1) that resulted in formation of the stable LuB_4 layer on the LuB_{12} crystal surface on heating in vacuum.

To clarify the origin of the LuB_4 thermionic properties with the emitting surface recovered by the LuB_2 phase that had been generated due to heating of LuB_4 during tests, the LuB_2 [001] single-crystal was grown and its thermionic properties were investigated in the temperature range of $T = 1200...1940$ K. At first temperature was increased to 1635 K during 5 h and then it was decreased to 1259 K during 1 h. The results of measurements showed the nonlinear $\varphi(T)$ dependence for LuB_2 (001)

(Fig. 4, c) and the larger thermionic current values compared with the current values of the LuB_2 layer generated on the LuB_4 sample. The highest thermionic current density was equal to 27 A·cm^{-2} ($\varphi = 2.30$ eV) at 1635 K. Taking into account that some metal diborides with AlB_2-type lattice are characterized by cationic non-stoichiometry [12] one can suppose that the preferential lutetium diffusion towards the surface from the near-surface layer takes place under LuB_2 heating that results in the thermionic current increase and electron work function decrease.

At the following stage the LuB_2 [001] annealing was carried out under $T = 1900$ K during 4 h. After annealing the obtained electron work function values were greater than before annealing (Fig. 4, c). According to the results of scanning electron microscopy with energy dispersive X-ray analysis the LuB_2 surface restructuring took place (Fig. 5, c). In doing so the individual boron layer approximately 0.3 μm in thick was formed at the crystal surface due to prefer-

ential lutetium evaporation and under this layer it was situated the layer enriched by boron approximately 5 μm in thick (Fig. 5, d). At the same time the X-ray phase analysis detected only LuB_2 (001) (insert in Fig. 5, c) because the boron layer of such size is transparent to X-rays.

The $\varphi(T)$ dependences for LuB_2 (001) both before annealing and after were obtained at temperature increase and decrease and they differ from each other (Fig. 4, c). The lower values of the electron work function correspond to the temperature decrease. Probable explanation of this phenomenon is that the temperature increase makes for increase of the lutetium diffusion velocity towards the surface resulting in the high metal concentration in the near-surface layer. With decreasing temperature the evaporation rate diminishes and the greater lutetium concentration defines the lower $\varphi(T)$ values.

For LuB_2 (001) the evaporation rate value is equal to $G = 8.6 \cdot 10^{-7}$ kg·m^{-2}·s^{-1} at $T = 1900$ K that practically amounts the G value for LuB_4 (001). This fact explains formation of the stable LuB_2 surface layer at the LuB_4 sample.

4. Conclusions

For the first time the thermionic properties of LuB_{12} (100), (110) and (111); LuB_4 (001) and LuB_2 (001) are studied. The electron work function of the LuB_{12} low-index planes increases in series $(100) \to (110) \to (111)$. This reduction correlates with a decrease of the reticular densities $d_r(B)/d_r(Er)$ ratio and an increase of the surface electric dipole moment in the same series. Preferential boron evaporation from the surfaces of LuB_{12} and LuB_4 borides results in the surface lutetium enrichment and hence the

thermionic current increase. This is supported by reduction of the electron work function under $LuB_{12} \to LuB_4$ and $LuB_4 \to LuB_2$ phase transformations on the surfaces of LuB_{12} and LuB_4 single crystals accordingly. LuB_2 (001) is characterized by the highest thermionic current density (27 A·cm^{-2} at $T = 1635$ K) among lutetium borides studied in this research and may be considered as perspective effective cathode material.

References

1. T.B.Massalski (Editor-in-Chief), Binary Alloy Phase Diagrams, 2-d ed. Plus Updates, ASM International, ASM CD-ROM, Ohio, USA (1996).
2. G.V.Samsonov, L.N.Okhremchuk, I.A.Podchernjaeva et al., *Izv. AN SSSR Neorg. Mater.*, **10**, 270 (1974).
3. D.Voronovich, A.Taran, N.Shitsevalova et al., *Solid State Sci.*, **14**, 1624 (2012).
4. H.Werheit, V.Filipov, K.Shirai et al., *J. Phys.: Condens. Matter.*, **23**, 065403 (2011).
5. R.Nishitani, M.Aono, T.Tanaka et al., *Surface Sci.*, **93**, 535 (1980).
6. L.W.Swanson, M.A.Gesley, P.R.Davis, *Surface Sci.*, **107**, 263 (1981).
7. D.A.Voronovich, A.A.Taran, N.Yu.Shitsevalova et al., *Aerospace Technic and Technology*, **4**, 80 (2011).
8. J.M.Lafferty, *J. Appl. Phys.*, **22**, 299 (1951).
9. V.S.Fomenko, Emission Properties of Materials, Naukova Dumka, Kiev (1981) [in Russian].
10. A.Taran, D.Voronovich, N.Shitsevalova et al., *Solid State Phen.*, **172–174**, 464 (2011).
11. L.N.Dobretsov, M.V.Gomoyunova, Emission Elektronics, Nauka, Moscow (1966) [in Russian].
12. A.L.Ivanovskii, I.R.Shein, N.I.Medvedeva, *Russ. Chem. Rev.*, **77**, 467 (2008).